FIRST RESULTS WITH HIFI

STUDIES OF EXTENDED ANOMALOUS EMISSION REGIONS WITH AN IMAGING FABRY-PEROT

R. Brent Tully
Institute for Astronomy, University of Hawaii

Jonathan Bland
University of Hawaii and Rice University

Gerald Cecil
Institute for Advanced Studies

ABSTRACT. The new imaging Fabry-Perot interferometer at the University of Hawaii is especially suited for studying extended emission regions in the vicinity of active nuclei. Dramatic results have been obtained for the objects observed so far: M51, M82, NGC 1068, NGC 4151, and NGC 4258.

HIFI: The Hawaii Imaging Fabry-Perot Interferometer

HIFI is an evolutionary derivative of imaging Fabry-Perot systems dating back to the sixties (Courtès 1964; Tully 1974; de Vaucouleurs and Pence 1980; Taylor and Atherton 1980; Williams, Caldwell, and Schommer 1984). It actually shares hardware with another Fabry-Perot system supported by the Canada-France-Hawaii Telescope, called CIGALE (Boulesteix et al. 1983).

All of these instruments are essentially very narrow band tunable filters, with the complexity that the filter transmission varies across the field of view. This complexity is not a severe problem in this age of image processing because the wavelength phase shift across the field can be calibrated to recover monochromatic images. The spectral filtering can be very narrow band indeed and our application with R=7000 represents no instrumental challenge.

As a reminder, the Fabry-Perot works by selectively transmitting only those wavelengths of light that bridge the gap between two highly reflecting surfaces in nearly an integral number of steps. The qualifier 'nearly' is described mathematically by the Airy function. Then the transmission properties of the etalon can be varied by changing the gap between reflecting plates. Figure 1 provides a representation of a constant phase surface in a raw data cube where the left-hand face of the cube corresponds to the response at a fixed etalon setting and the direction along the axis of the paraboloids corresponds to change in the spacing of the reflecting surfaces of the etalons. Nowadays, the Fabry-Perot systems of choice are the piezoelectric scanned, capacitance stabilized units built by Queensgate Instruments (Hicks, Reay, and Atherton 1984).

With a magic wand (Bland and Tully 1988b), the raw data cube can be transformed into the format schematicized in Figure 2. The x-y plane corresponds to the field-of-view. The separate z surfaces correspond to increments in wavelength or velocity, which for a study of active nuclei

D. E. Osterbrock and J. S. Miller (eds.), Active Galactic Nuclei, 337–342.

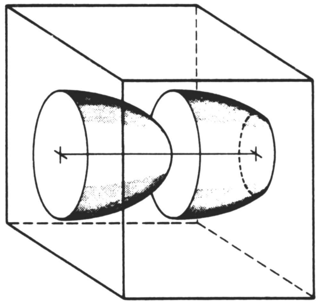

Fig. 1
Constant phase surfaces in a raw data cube. Horizontal dimension is scan direction. Surfaces of maximum transmission for monochromatic light are illustrated through almost two orders.

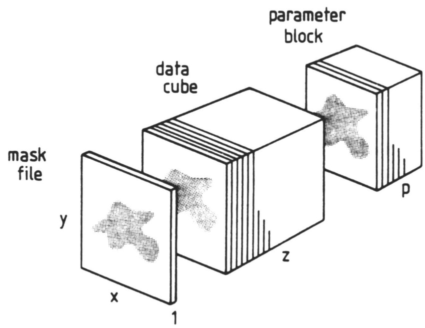

Fig. 2
Phase corrected data cube. The mask file delineates a region of interest on the sky. The data cube contains intensities at x-y spatial locations and z spectral channels. Information characterizing the profiles at each x-y position are stored in the parameter block.

might be chosen to be 35 km/s. Then the profile at each x-y pixel might be characterized in the parameter block. Some of the parameters we save are profile peak velocity, line width, line skewness, line intensity, continuum intensity, line percent polarization and polarization orientation, and ratio of the intensities of separate lines. Sometimes line profiles are sufficiently complex that more sophisticated characterizations are required.

Our instrument has two advantages over Fabry-Perot predecessors for the study of active nuclei:

1. With our CCD, we have a geometrically stable and linear photometric detector. We can intersperse spectral calibrations and acquire complete flat-field mapping of the response of the system including isolation filter. Consequently, we end up with extremely high signal-to-noise spectra with good quality kinematic and photometric information.

2. We use an etalon that gets around the problem of interorder confusion. Working in low order (around 75 at 6600 Å), we have a free-spectral-range of 4000 km/s. Adjacent orders can be blocked with an interference filter. A satisfactory spectral resolution of FWHM = 70 km/s is retained by using particularly highly reflecting etalon surfaces, producing a 'finesse' of about 60.

Early Results

M 51 was the first object we studied and, being the first, it was less than optimally sampled. The work has been discussed by Cecil (1988). There is a close affiliation between the morphology of high excitation [NII] λ6583 in the nuclear region and non-thermal radio emission

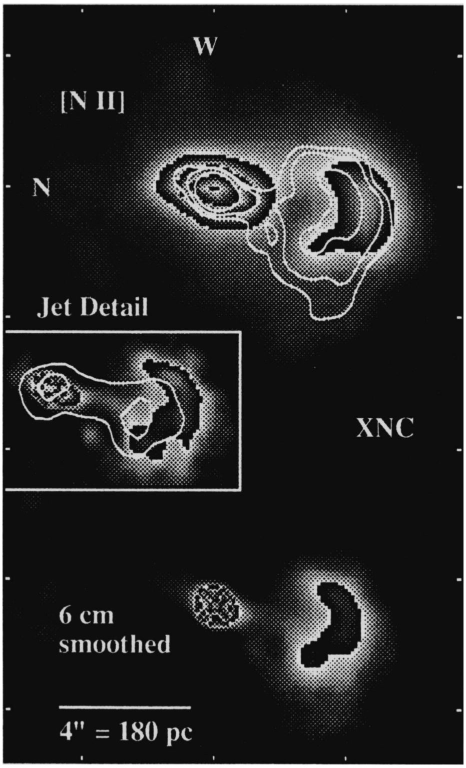

Fig. 3
The extranuclear cloud in M51. Bottom: λ6cm VLA map smoothed to resolution of Fabry-Perot observations. Region of highest intensity is nucleus and XNC is 4" south. Top: [NII] channel at +100 km/s with VLA contours superimposed. Peak radio emission is slightly inside [NII] emission near systemic. Insert: λ6cm VLA map with 0".5 resolution and + 580 km/s channel map contours superimposed. High velocity gas is displaced inward with respect to XNC and coincides with apparent radio jet. VLA observations by Crane et al.

mapped with the VLA (Ford et al. 1985; Crane et al. 1987). Cecil focused on the physics of the 'extranuclear cloud', a region 4 arcsec from the nucleus with the broadest and most complex emission profiles in the system. It is associated with a working surface where collimated relativistic particles from the nucleus impinge on ambient material. Distinct velocity components are seen at -180 and +450 km/s with respect to systemic. Unusual excitation conditions are found in the barely resolved region, with [NII]λ6583 /Hα reaching a value of five. Cecil developed a model in which relativistic particles from the nucleus have deposited energy at the working surface, driving 500 km/s shock fronts in the ambient medium for us to observe.

https://doi.org/10.1017/S0074180900141269 Published online by Cambridge University Press

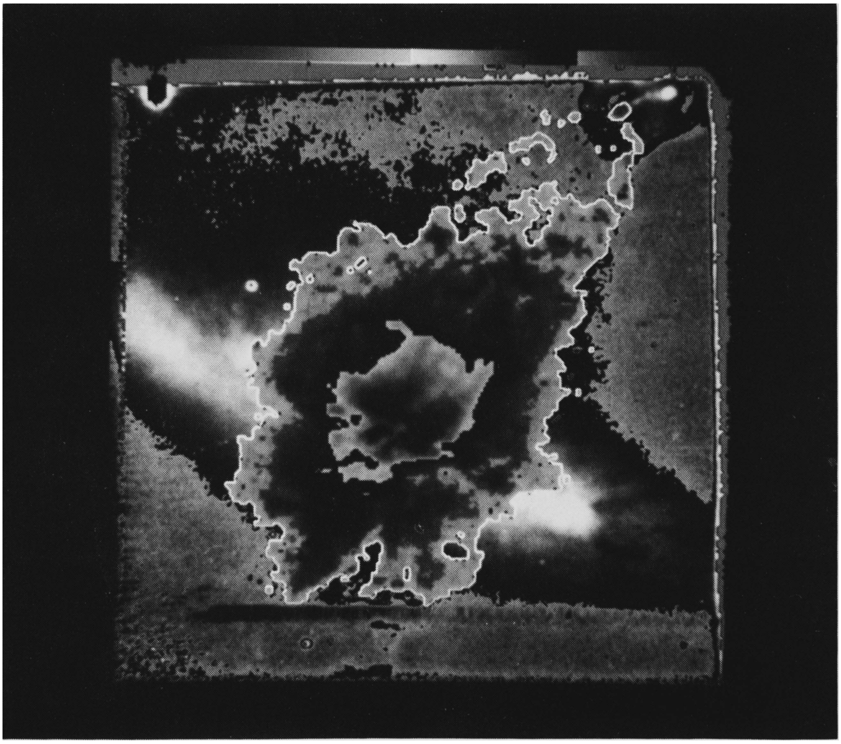

Fig 4.
Hα image of M82 superimposed on a continuum image. The continuum-subtracted line emission has been masked, then inserted into an image of the continuum flux. We model the outward moving gas on the minor axis in terms of a supernova driven galactic wind.

As can be seen in Figure 4, our data on M 82 are visually spectacular. In spite of the chaotic appearance of the galaxy, the velocity field turns out to have remarkable symmetries that can be explained in terms of a simple model (Bland and Tully 1988a). Three distinct components of emission are identified:

1. Gas in the plane of the galaxy is in orderly rotation. The rotation curve is flat at about 100 km/s outside a radius of about 10" = 150 pc.

2. The dramatic filamentary emission along the minor axis (Lynds and Sandage 1963) is observed to have velocities that monotonically increase with distance to achieve line-of-sight values of $\pm$400 km/s, probably corresponding to deprojected values of 600 km/s. The profiles are split in well-defined regions (see also Axon and Taylor 1978) strongly indicating we are seeing emission from surfaces of bubbles. There is x-ray emission from within the bubbles (Watson, Stanger, and Griffiths 1984). It is interpreted that we see cool sheaths on bubbles due to galactic winds driven by supernovae in the central regions (Kronberg and Sramek 1985; Chevalier and Clegg, 1985). The bubbles have been collimated toward the poles by the disk interstellar medium.

3. Weak, but omnipresent within 2 kpc, is a diffuse halo of emission with broad line profiles (300 km/s) and relatively high excitation ([NII] / Hα = 0.8). We suspect that this component gives rise to the known polarized radiation (Elvius 1963; Sandage and Miller 1964; Solinger 1969). The broad line and polarized continuum radiation might be light from a nuclear starburst reflected to us by a halo of dust particles.

The other galaxy we have studied in detail is NGC 1068. Separate presentations by Cecil on the central region and Bland on the large-scale disk are given at this conference.

The final figure (Fig. 5) is a preliminary Hα image of the south side of NGC 4258. The anomalous Hα arm discovered by Courtès and Cruvellier (1961) which corresponds to the nonthermal radio feature mapped by van der Kruit, Oort, and Mathewson (1972) is clearly seen. We will soon have maps of the velocity field and excitation conditions of this unusual feature.

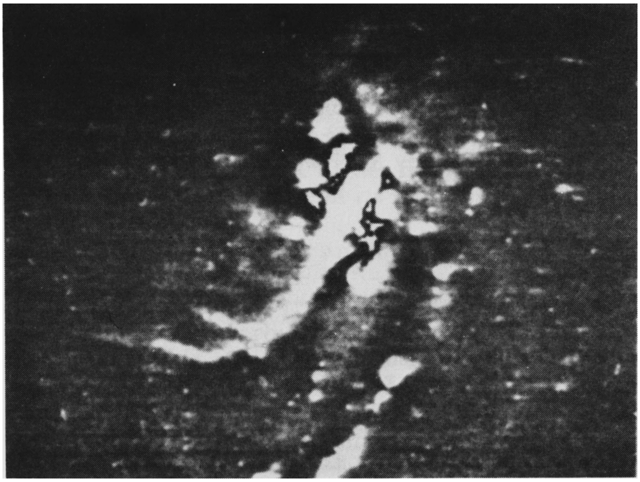

Fig 5.
Stacked channel maps of the south side of NGC 4258, after unsharp mask removal of low spatial frequencies. The anomalous Hα arm associated with nonthermal radio emission extends from the nuclear region toward the lower left. The emission knots extending to the edge of the field at the bottom are associated with normal spiral arms.

Additional Comments

Apparently, large-scale non-gravitational motions occur commonly in galaxies. These phenomena are poorly studied because they tend not to involve the neutral gas that can be observed with synthesis radio telescopes and because optical spectroscopic techniques have hitherto not provided efficient spatial coverage. The more complicated the situation, the more necessary is complete two-dimensional coverage, and the greater the advantage provided by the imaging Fabry-Perot. In the case of extended anomalous emission associated with active nuclei,

https://doi.org/10.1017/S0074180900141269 Published online by Cambridge University Press

two-dimensional coverage is vital. It is a futile exercise to anticipate the nature of the anomalies and only partially sample the available space with a slit spectrograph.

A frequent comment made only partially in jest concerns the very large amount of data generated by the instrument. There is trepidation that the amount of information might be so overwhelming as to be indigestible. The problem is exacerbated by the limited resources available for optical programs, in contrast with the team approach practised in, say, radio astronomy. While these concerns have a real basis, it must also be true that there are more rational ways of ignoring 99% of the available information than by laying down a slit. In our preliminary studies, we have not been able to give proper attention to the bulk of our data, but just having access to the 'big picture' has allowed us to see simplifying symmetries (the orderly outflow and systematic pattern of line splitting in the bipolar bubbles of M 82; the two arm spiral symmetry in the velocity pattern of NGC 1068), or to detect large-scale correlations (the marked morphological similarities between nonthermal radio and high excitation line emission in M 51 and NGC 1068; the omnipresence of high excitation gas of faint emissivity in M 82 and NGC 1068), or to isolate regions of special interest (the extranuclear cloud in M 51; the region of the jets in NGC 1068).

Nevertheless, it is true that there is too much information produced for our small group to absorb in a reasonable amount of time. Our rule-of-thumb is that order 1 night of observing requires order 10 days to reduce and order 100 days to understand. There is room for more hands. Our software is portable to any SUN workstation or to UNIX systems in general. Collaborations are possible.

References

Axon, D. J., and Taylor, K. 1978, *Nature*, **274**, 37.
Bland, J., and Tully, R. B. 1988a, *Nature*, **334**, 43.
Bland, J., and Tully, R. B. 1988b, *A. J.*, (submitted).
Boulesteix, J., Georgelin, Y. P., Marcelin, M., and Monnet, G. 1983, *SPIE Conf. Inst. Astron. V*, **445**, 37.
Cecil, G. N. 1988, *Ap. J.*, **329**, 38.
Chevalier, R.A. and Clegg, A.W., *Nature*, **317**, 44.
Crane, P. C., van der Hulst, J. M., Ford, H. C., Lawrie, D. G., and Jacoby, G. H. 1987, *Bull. A. A. S.*, **19**, 681.
Courtès, G. 1964, *A. J.*, **69**, 325.
Courtès, G., and Cruvellier, P. 1961, *Comtes Rendus Acad. Sci. Paris*, **253**, 218.
de Vaucouleurs, G., and Pence, W. D. 1980, *Ap. J.*, **242**, 18.
Elvius, A. 1963, *Lowell Obs. Bull.*, **5**, 281.
Ford, H. C., Crane, P. C., Jacoby, G. H., Lawrie, D. G., and van der Hulst, J. M. 1985, *Ap. J.*, **293**, 132.
Hicks, T. R., Reay, N. K., and Atherton, P. D. 1984, *J. Phys. E.*, **17**, 49.
Kronberg, P. P., and Sramek, R. A. 1985, *Science*, **227**, 28.
Lynds, C. R., and Sandage, A. 1963, *Ap. J.*, **137**, 1005.
Sandage, A., and Miller, W. C. 1964, *Science*, **144**, 405.
Solinger, A. B. 1969, *Ap. J.*, **155**, 403.
Taylor, K., and Atherton, P. D. 1980, *M. N. R. A. S.*, **191**, 675.
Tully, R. B. 1974, *Ap. J. Suppl.*, **27**, 415.
van der Kruit, P. C., Oort, J. H., and Mathewson, D. S. 1972, *Astr. Ap.*, **21**, 169.
Watson, M. G., Stanger, V., and Griffiths, R. E. 1984, *Ap. J.*, **286**, 144.
Williams, T. B., Caldwell, N., and Schommer, R. A. 1984, *Ap. J.*, **281**, 579.